Synthesis, Structural Characterization, and Magnetic Study of $Sr_4Mn_2CoO_9$

K. Boulahya,† M. Parras,† J. M. González-Calbet,*,† and J. L. Martínez‡

Departamento de Química Inorgánica, Facultad de Químicas, Universidad Complutense, E-28040-Madrid, Spain, and Instituto de Ciencia de Materiales, CSIC, Cantoblanco, E-28049-Madrid, Spain

Received March 7, 2003. Revised Manuscript Received June 5, 2003

Polycrystalline $Sr_4Mn_2CoO_9$ has been synthesized and characterized by X-ray and electron diffraction, high-resolution electron microscopy, and magnetic measurements. This oxide constitutes the $\alpha = 3, \beta = 1$ term of the homologous series $(A_3B_2O_6)_\alpha(A_3B_3O_9)_\beta$. The essential feature of this structure is the presence of isolated rows of polyhedra sharing faces along the *c*-axis and formed by the alternation of one trigonal prism occupied by a Co cation and two Mn cations in octahedral coordination; the chains are separated by Sr atoms. The magnetic properties seem to indicate strong antiferromagnetic correlations along the chains, but no three-dimensional (3D) magnetic long range order is observed. The global magnetic behavior indicates a partially ordered system, close to a magnetic spin glass.

Introduction

Prompted by the intriguing magnetic properties of one-dimensional oxides related to the 2H−$BaNiO_3$[1] structure, considerable work on their structural control has been recently carried out, especially on those materials exhibiting a transition to a 3D magnetic ordered state. This is the case for $Ca_3Co_2O_6$,[2] which crystallizes in the K_4CdCl_6[3] structural type, formed by an oriented hexagonal array of ferromagnetically coupled chains constituted by alternating face-sharing [CoO_6] octahedra (O_h) and [CoO_6] trigonal prisms (TP). Interchain magnetic coupling is antiferromagnetic, with ferromagnetic 3D ordering being reached below 13 K. Each chain is surrounded by six parallel one-dimensional neighboring chains containing Ca atoms. The substitution of Co by Rh in octahedral sites results in an isostructural Ca_3CoRhO_6[4,5] material showing a partially disordered antiferromagnetic state at low temperature.

The ability of both 2H−$BaNiO_3$ and K_4CdCl_6 structural types to intergrow in an ordered way has played a paramount role in the stabilization of new one-dimensional oxides with different octahedral/trigonal prism ratios.[6] Actually, all of them can be described as members of the $(A_3A'BO_6)_\alpha(A_3B_3O_9)_\beta$[7] homologous series in which B stands for octahedrally coordinated cations and A′ refers to cations in TP environment. The ionic radius of the alkaline-earth occupying A sites governs, in some way, the O_h/TP ratio: the larger the radius the higher is the ratio. Both the high number of octahedra and the bigger size of the alkaline-earth thwart the 3D ordering because the intrachain and interchain coupling is more difficult to achieve, thus leading to paramagnetic behavior as in $Ba_8CoRh_6O_{21}$.[8]

Considering that the smaller size of the cations together with the smaller O_h/TP ratio enhances the magnetic cation coupling, intermediate members of the above-mentioned homologous series have been explored. $Sr_{3.3}Ca_{0.7}CoRh_2O_9$,[9] the $\alpha = 3\ \beta = 1$ member, is formed by two face-sharing octahedra alternating to one trigonal prism running parallel to the *c*-axis and shows weak antiferromagnetic interaction between magnetic cations. In the case of two transition metals of the first series in O_h and TP sites, an isostructural oxide has been stabilized for $Sr_4Mn_2NiO_9$.[10] Mn occupies the octahedra and Ni is disordered in the TP with 80% in the pseudo square faces of the prism and 20% at the center. This particular characteristic affects both the microstructure and magnetic behavior. Actually, on one hand, the cationic arrangement into the trigonal prismatic sites seems to create a disordered situation reflected in the formation of multitwinned domains in all crystals, as also observed in $Sr_9Mn_5Ni_2O_{21}$[11] or $Sr_4Mn_2CuO_9$.[12] On the other hand, the magnetic behavior is also determined by such a displacement. In this sense, the

* Corresponding author. E-mail: jgcalbet@quim.ucm.es. Phone: (34) 91 394 43 42/58. Fax: (34) 91 394 43 22.
† Universidad Complutense.
‡ Instituto de Ciencia de Materiales, CSIC.

(1) Lander, J. J. *Acta Crystallogr.* **1951**, *4*, 148.
(2) Fjellvag, H.; Gulbrandse, E.; Aasland, S.; Olsen, A.; Hauback, B. C. *J. Solid State Chem.* **1995**, *5*, 557.
(3) Bergerhoff, G.; Schmitz-Dumont, O. *Z. Anorg. Allg. Chem.* **1956**, *10*, 284.
(4) Niitaka, S.; Kageyama, H.; Kato, M.; Yoshimura, K.; Kosuge, K. *J. Solid State Chem.* **1999**, *146*, 137.
(5) Niitaka, S.; Yoshimura, K.; Kosuge, K.; Shi, M. N.; Kakurai, K. *Phys. Rev. Lett.* **2001**, *87*, 177202.
(6) . Darriet, J.; Subramanian, M. A. *J. Mater. Chem.* **1995**, *5*, 543.
(7) Boulahya, K.; Parras, M.; González-Calbet, J. M. *Chem. Mater.* **2000**, *12* (1), 25.
(8) Zur Loye, H.-C.; Stizer, K. E.; Smith, M. D. *Inorg. Chem.* **2001**, *40*, 5152.
(9) Hernando, M.; Boulahya, K.; Parras, M.; Varela, A.; González-Calbet, J. M.; Martínez, J. L. *Chem. Mater.* **2002**, *14*, 4948.
(10) El Abed, A.; Gaudin, E.; Lemaux, S.; Darriet, J. *Solid State Sci.* **2001**, *3*, 887.
(11) Hernando, M.; Boulahya, K.; Parras, M.; González-Calbet, J. M.; Amador, U. *Eur. J. Inorg. Chem.* **2003**, 2419.
(12) El Abed, A.; Gaudin, E.; Darriet, J. *Acta Crystallogr.* **2002**, *C58*, i138.

10.1021/cm034130t CCC: $25.00
Published on Web 08/02/2003

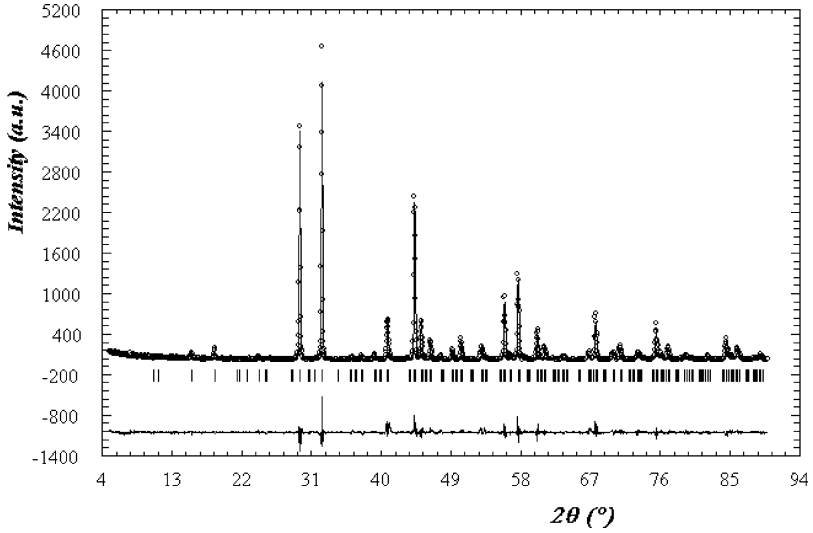

Figure 1. Experimental, calculated, and difference X-ray diffraction pattern for $Sr_4Mn_2CoO_9$.

temperature dependence of the magnetic susceptibility in $Sr_4Mn_2NiO_9$[13] can be explained by a model in which the solid is constituted by two sublattices: a paramagnetic one formed by a random distribution of the small fraction of Ni^{2+} centered in the TP sites, and a Mn^{4+} ionic-sublattice in which $[Mn_2O_6]$ dimmers are antiferromagnetically coupled. These sublattices are nearly independent, hence, the 3-D antiferromagnetic ordering is achieved at low temperature (T_N = 3 K) through interchain interactions in the Mn^{4+} sublattice.

The replacement of Ni by Co in analogous 1D-oxides modifies both structural and magnetic characteristics. In the case of Ca_3MnCoO_6,[14] where Mn occupies the octahedra and Co is at the TP center, no multitwinning appears. We describe in this paper the synthesis, structural characterization, and magnetic properties of the $\alpha = 3$, $\beta = 1$ member of the homologous series $(A_3A'BO_6)_\alpha(A_3B_3O_9)_\beta$ with the composition $Sr_4Mn_2CoO_9$.

Experimental Section

Polycrystalline $Sr_4Mn_2CoO_9$ was synthesized by heating stoichiometric amounts of $SrCO_3$ (Aldrich 99.98%), Co_3O_4 (Aldrich 99+%), and MnO_2 (Aldrich 99+%) in air at 1275 °C for 5 days and then quenching to room temperature.

Powder X-ray diffraction (XRD) patterns were collected with Cu Kα radiation at room temperature on a PHILIPS X'PERT diffractometer equipped with a graphite monochromator. The diffraction data were analyzed by the Rietveld method using the Fullprof program.

The sample was characterized by SAED and HREM carried out in a JEOL 3000 FEG electron microscope, fitted with a double tilting goniometer stage (±22°, ±22°). Local composition was analyzed with an INCA analyzer system attached to the above microscope. Simulated HREM images were calculated by the multislice method using the MacTempas software package.

Magnetic properties were measured in a SQUID magnetometer, in a temperature range from 1.7 to 400 K, and under magnetic fields up to 50 kOe for polycrystalline samples. The specific heat was measured by the heat pulse-relaxation method in a commercial cryostat (PPMS, from Quantum Design, San Diego, CA) with a temperature range from 1.7 to 300 K and magnetic fields up to 90 kOe. A pellet of the sample (approximately 15 mg) was attached to a sapphire platform by a small amount of Apiezon N grease. The addenda heat capacity was measured in a separate run and subtracted from the sample data.

Results and Discussion

The cationic composition, as analyzed by inductive coupling plasma and energy-dispersive X-ray analysis, is in agreement with the nominal composition. The X-ray diffraction pattern (Figure 1) can be indexed on the basis of a trigonal unit cell with lattice parameters a = 9.5852(7) Å and c = 7.8266(4) Å, with no extra reflections being detected.

Selected area electron diffraction (SAED) has been used to fully reconstruct the reciprocal space, confirming the above unit cell. Reflection conditions are compatible with space group $P321$ (150), in agreement with the space group of $(Sr_{0.5}Ca_{0.5})_4Co_3O_9$.[15] The most relevant reciprocal zone axis, $[1\bar{2}10]$, is shown in Figure 2a. The corresponding HREM micrograph (Figure 2b) shows an apparently well ordered material with d spacings of 8.3 and 7.8 Å, corresponding to d_{100} and d_{001}. The contrast observed in this image corresponds to three bright dots alternating with a brighter one folded along the c-axis, which can be associated with the Sr configuration shown in the structural model depicted in Figure 3. Therefore, from the refined atomic coordinates of $Sr_4Mn_2CoO_9$ (see the next section), an image calculation was performed. The simulated image fits nicely to the experimental one at Δt = 30 Å and $\Delta f = -40$ Å. It is worth emphasizing that the SAED study gives no evidence of multitwinning in this material.

On the basis of the above results, an X-ray profile refinement of $Sr_4Mn_2CoO_9$ was performed by the Rietveld method[16] using the Fullprof program[17] taking as starting point the $(SrCa)_4Co_3O_9$ crystallographic data. In this structure model, cobalt atoms are distributed over five crystallographic positions, two of which present trigonal prismatic coordination while the other three correspond to octahedral oxygen environment. In

(13) El Abed, A.; Gaudin, E.; Darriet, J.; Whangbo, M. H. J *J. Solid State Chem*. **2002**, *163*, 513.
(14) Zubkov, V. G.; Bazuev, G. V.; Tyutyunnik A. P.; Berger, I. F. *J. Solid State Chem*. **2001**, *160*, 293.
(15) Boulahya, K.; Parras, M.; González-Calbet, J. M. *J. Solid State Chem*. **1999**, *145*, 166.
(16) Rietveld, H. V. *J. Appl. Crystallogr*. **1969**, *2*, 65.
(17) Rodríguez-Carvajal, J. *J. Physica* **1993**, *B192*, 55.

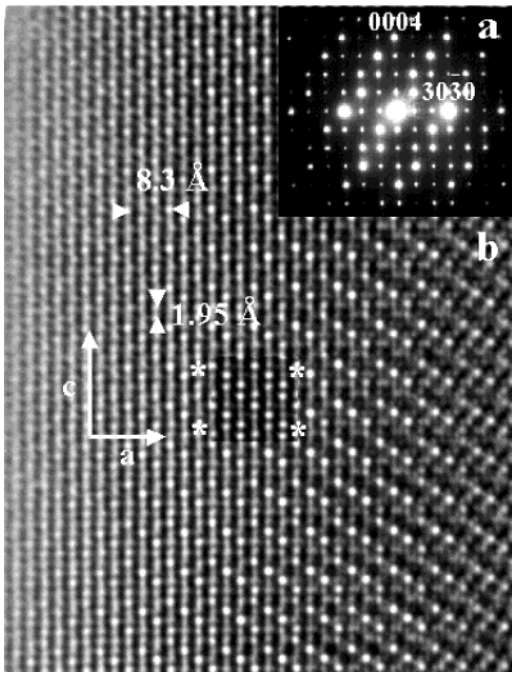

Figure 2. (a) SAED pattern of $Sr_4Mn_2CoO_9$ along [1$\bar{2}$10]. (b) Corresponding HRTEM image. Simulated image is shown in the inset.

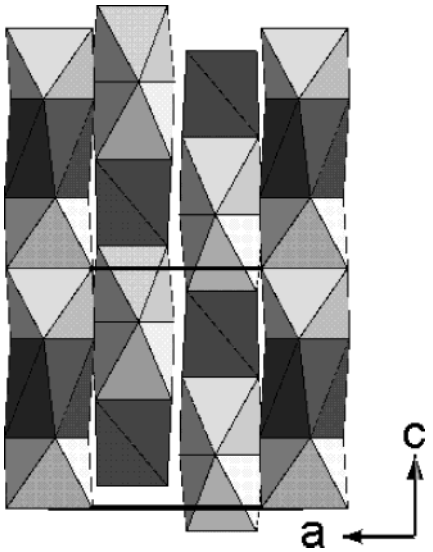

Figure 3. Structural model of $Sr_4Mn_2CoO_9$ along *b* axis.

$Sr_4Mn_2CoO_9$, Co and Mn atoms are arranged in the TP and octahedral sites, respectively. Peak shapes were described by pseudo-Voigt functions. Figure 1 shows the graphic results of the fitting of the experimental X-ray diffraction pattern and the difference between observed and calculated data. The refinement was stable and it was possible to refine the positions of oxygen atoms, provided a temperature factor for each type of atom was used. Any attempt to use individual temperature factors yielded unstable refinements, probably due to the high number of refined parameters, preferred orientation (10%), and the limited number of observed reflections (588). The final structural parameters are collected in Table 1, whereas Table 2 shows some selected inter-atomic distances. The structure refinement confirms isotypism with $(SrCa)_4Co_3O_9$. The essential feature of the structure is the presence of rows of polyhedra formed by the alternation of Co trigonal prism and two Mn

Table 1. Final Structural Parameters of $Sr_4Mn_2CoO_9$[a]

atom	*x*/*a*	*y*/*b*	*z*/*c*	$B_{iso}(Å^2)$
Sr1	0.0242(9)	0.6902(9)	0.249(3)	1.063(6)
Sr2	0.345(2)	0.00000	0.50000	1.063(6)
Sr3	0.327(2)	0.00000	0.00000	1.063(6)
Mn1	0.00000	0.00000	0.165(4)	1.58(17)
Mn2	0.33333	0.66667	0.069(5)	1.58(17)
Mn3	0.33333	0.66667	0.377(5)	1.58(17)
Co2	0.00000	0.00000	0.50000	1.58(17)
Co1	0.33333	0.66667	0.721(9)	1.58(17)
O1	0.490(7)	0.653(5)	0.25(1)	0.40(29)
O2	0.652(9)	0.178(9)	0.456(6)	0.40(29)
O3	0.835(10)	0.00000	0.00000	0.40(29)
O4	0.660(9)	0.193(7)	0.089(6)	0.40(29)
O5	−0.035(6)	0.148(8)	0.303(7)	0.40(29)

[a] Space group *P*321 (150); $a = 9.5852(7)$ Å; $c = 7.8266(4)$ Å; $V = 622.732(2)$ Å^3; $R_B = 0.069$; $R_{exp} = 0.106$; $R_{wp} = 0.180$; $\chi^2 = 2.85$.

Table 2. Selected Inter-Atomic Distances Less than 3.0 Å in $Sr_4Mn_2CoO_9$

Sr1−O1: 2.687 (6)	Mn1−O3: 2.04 (4) × 3
O1: 2.652 (6)	O5: 1.94 (6) × 3
O2: 2.584 (7)	Mn2−O1: 2.13 (8) × 3
O2: 2.857 (7)	O4: 1.81 (8) × 3
O3: 2.470 (4)	Mn3−O1: 1.85 (6) × 3
O4: 2.456 (7)	O2: 1.92 (8) × 3
O5: 2.527 (7)	Co1−O2: 1.98 (8) × 3
O5: 2.899 (7)	O4: 1.97 (8) × 3
Sr2−O1: 2.481 (8) × 2	Co2−O5: 2.22 (5) × 6
O2: 2.583 (9) × 2	Mn1−Mn1: 2.58 (5)
O2: 2.907 (9) × 2	Co2: 2.62 (3)
O5: 2.328 (6) × 2	Mn2−Mn3: 2.41 (6)
Sr3−O1: 2.596 (8) × 2	Co1: 2.73 (6)
O3: 2.710 (9) × 2	Mn3−Co1: 2.69 (6)
O4: 2.869 (8) × 2	
O4: 2.928 (5) × 2	
O5: 2.851 (4) × 2	

octahedra separated by Sr atoms and folded along [0001] direction. The inter-cation distances Mn−Mn (2.41(6)−2.58(5) Å) and Mn−Co (2.62(3)−2.73(6) Å) within the polynuclear ($CoMn_2O_9$) group agree well with those of similar oxides also containing face-sharing polyhedra, such as $Sr_4Mn_2NiO_9$ (2.556−2.572 Å), $Sr_7Mn_4O_{15}$[18] (2.53 Å), or Ca_3MnCoO_6 (2.645 Å). These geometrical conditions will determine the magnetic behavior (see below). The Mn−O distances of 1.85(6) and 2.13(8) Å are typical for Mn^{4+} octahedra in oxides $Sr_4Mn_3O_{10}$[19] (1.77−2.10 Å) or $Sr_7Mn_4O_{15}$ (1.83−2.05 Å). Finally, the Sr−O distances (2.328(6)− 2.928(5) Å) are close to those observed in other Sr oxides, for instance, d(Sr−O) = 2.36−3.02 Å in $Sr_7Mn_4O_{15}$.

The ensemble of the XRD, SAED, and HREM results shows that $Sr_4Mn_2CoO_9$ constitutes a new example of a 1D-oxide where 1TP is stacked to two octahedra along the *c*-axis. Besides, the structure refinement shows that Co atoms are located at the center of the TP sites (see Table 1). Thus, in relation to the above-mentioned $Sr_4Mn_2NiO_9$,[10] $Sr_9Mn_5Ni_2O_{21}$,[11] or $Sr_4Mn_2CuO_9$[12] multitwinned phases, a more ordered situation is attained and no extended defects have been evidenced by SAED or HREM. The same structural features have been observed in Ca_3MnCoO_6.[14]

Different physical properties also have been explored. First, the sample is an electrical insulator below room

(18) Vente, J. F.; Kamenev, K. V.; Sokolov, D. A. *Phys. Rev. B* **2002**, *64*, 214403.
(19) Floros, N.; Hervieu, M.; van Tendeloo, G.; Michel, C.; Maignan, A.; Raveau, B. *Solid State Sci.* **2000**, *2*, 1.

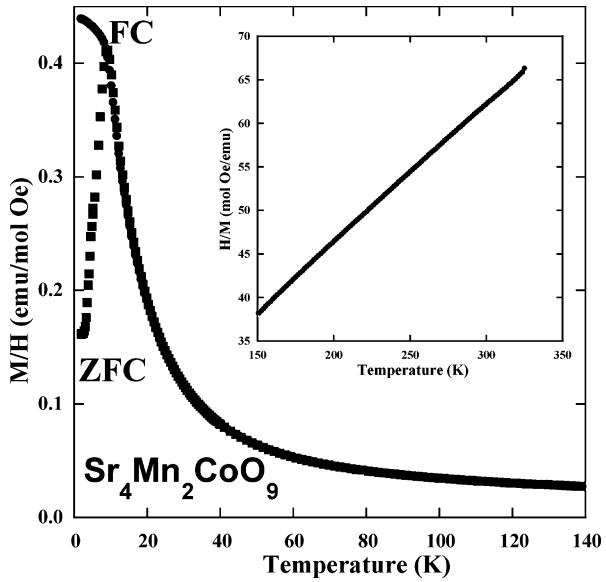

Figure 4. Temperature dependence of the magnetic susceptibility after zero field cooling and field cooling (H = 1 kOe). The inset shows the temperature dependence of the inverse magnetic susceptibility.

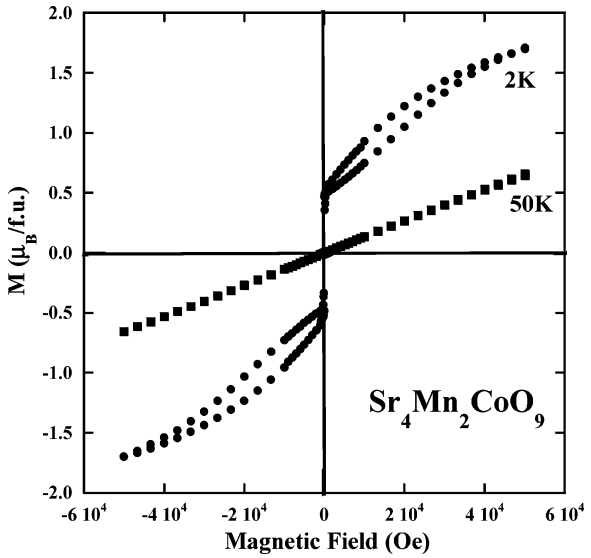

Figure 5. Magnetization curves versus applied magnetic field at different temperatures (2 and 50 K).

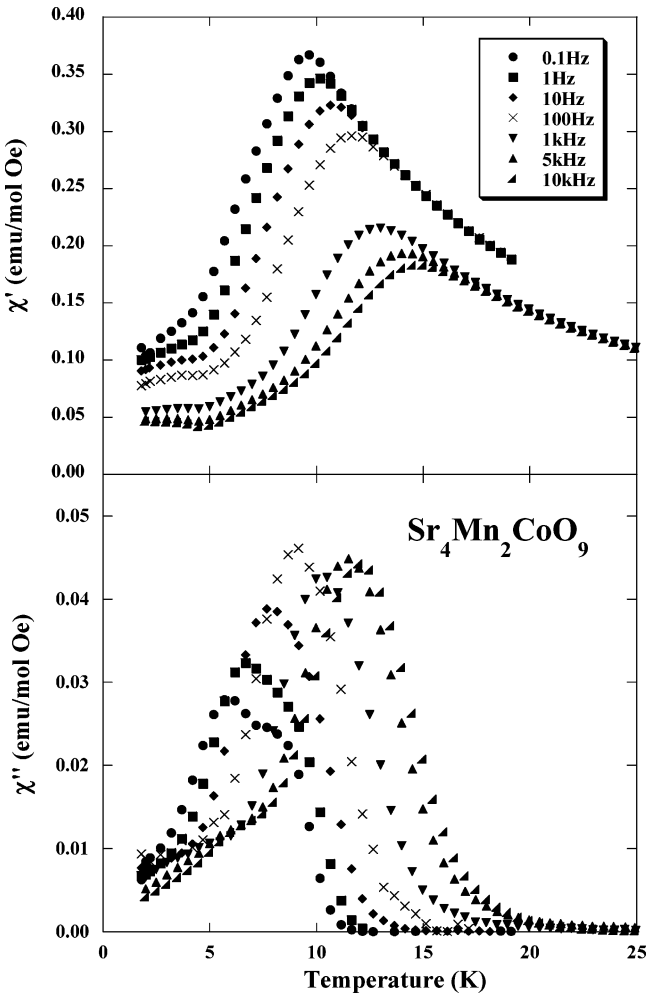

Figure 6. Upper frame: Temperature dependence of the real part of the ac magnetic susceptibility at different frequencies from 0.1 Hz to 10 kHz. Lower frame: Imaginary part of the ac magnetic susceptibility at the same frequencies.

temperature. The magnetic properties are presented in Figure 4. The magnetic susceptibility of $Sr_4Mn_2CoO_9$ presents a strong dependence on the zero field cooling vs. field cooling process, with a clear maximum of irreversibility from 9.5 K. The inverse of the magnetic susceptibility follows a Curie−Weiss law in a range from 150 to 300 K, with an effective paramagnetic moment, calculated from the slope, of 7.1 μ_B/formula unit for an expected value of 7.8 μ_B/formula unit. This value agrees rather well with the assumption of two Mn^{4+} (3.8 μ_B/Mn) and one Co^{2+} (4.8 μ_B/Co). The calculated Weiss constant $\Theta = -91$ K indicates clearly that the predominant magnetic interactions are antiferromagnetic in origin. Taking into account the geometrical description of the crystallographic structure, the rows are formed by pairs of Mn^{4+} ions in the octahedral sites and the Co^{2+} ion in the trigonal prism site. In the temperature range from 150 to 300 K, the two Mn ions will tend to correlate antiferromagnetically (due to the short distance). However, no long range 3D antiferromagnetic order is achieved through the Co ion. Similar behavior was observed in Ca_3MnCoO_6[14], but, in this latter case, an antiferromagnetic order is obtained at T_N 13 K. In our case, when the temperature decreases, the system freezes with a random distribution of magnetic interactions (between chains), arriving at a disordered magnetic state at low temperature. Figure 5 shows the hysteresis loops at two temperatures, below and above the magnetic susceptibility irreversibility temperature. At high temperature (50 K) the behavior corresponds to a paramagnetic system. At low temperature (2 K) the magnetization curve presents a sharp increase at low magnetic fields (50 Oe), followed by a hysteretic behavior without reaching a saturation. To shed some light on the magnetic character of $Sr_4Mn_2CoO_9$, a.c. magnetic susceptibility measurements over a wide range of frequencies (0.1 Hz to 10 kHz) were performed. The data presented in Figure 6 show that the maximum in the real part of the magnetic susceptibility is displaced from 9.5 K (0.1 Hz) to 15 K (10 kHz). Also, there is a strong dispersion at the different frequencies below the susceptibility peak, but all the frequencies coincide for temperatures above the maximum. A clear peak (frequency dependent) is observed in the imaginary part of the magnetic susceptibility, ranging from 9 to 15 K. Figure 7 shows the temperature dependence of the a.c.

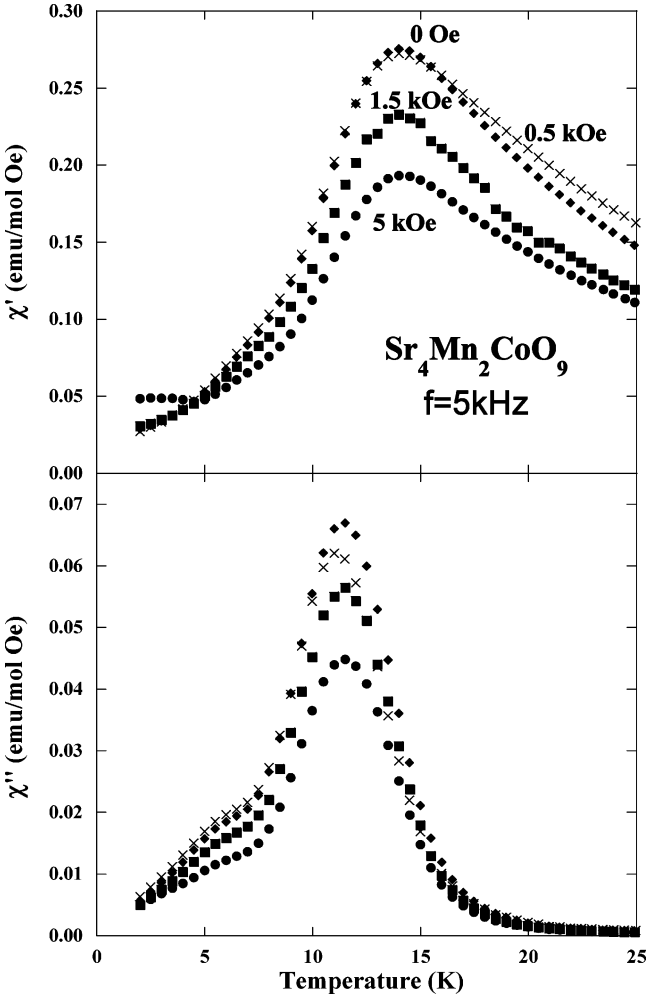

Figure 7. Upper frame: Temperature dependence of the real part of the ac magnetic susceptibility at different applied magnetic fields at a fixed frequency of 5 kHz. Lower frame: Imaginary part of the ac magnetic susceptibility at the same magnetic fields.

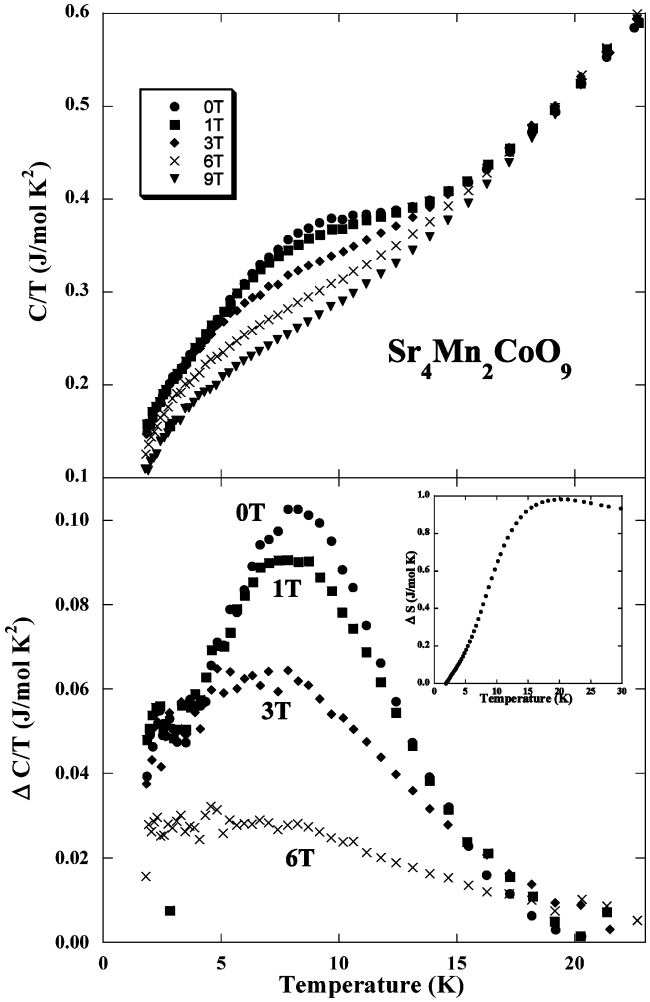

Figure 8. Upper frame: Temperature dependence of the specific heat for $Sr_4Mn_2CoO_9$, at different magnetic fields up to 9 T. Lower frame: Magnetic specific heat versus temperature. The inset shows the temperature dependence of the magnetic entropy at zero magnetic field for $Sr_4Mn_2CoO_9$.

magnetic susceptibility (fixed frequency of 5 kHz) on the applied external magnetic field. Both (real and imaginary) parts of the magnetic susceptibility decrease with the applied magnetic field, keeping constant the temperature of the maximum. According to these magnetic results, $Sr_4Mn_2CoO_9$ behaves as a partially disordered system. This behavior could be similar to that described in the case of Ca_3CoRhO_6[5] These results are different from those observed in the antiferromagnetic isostructural $Sr_4Mn_2NiO_9$.[13] In this latter case, the pairs of Mn^{4+} ions in the chains are antiferromagnetically coupled along the chains, and finally at low temperatures the different chains are coupled antiferromagnetically with long range order at $T_N = 3$ K.

The low-temperature specific heat at different applied magnetic fields for $Sr_4Mn_2CoO_9$ is presented in Figure 8 (upper frame). The total specific heat should have at least three components: electronic, magnetic, and lattice (phonons). In our case the first one should be negligible (insulator). The lattice component should follow a Debye model (αT^3) in this temperature range. To separate the different components is rather complicated. To extract the magnetic part of the specific heat we performed the same experiment at different magnetic fields up to 9 T. This field (9 T) is expected to be strong enough to keep aligned the magnetic ions in this temperature range (up to 30 K), so that the variation in entropy will be very small. This could be the case because the system stays in either a paramagnetic or a spin glass low temperature state. Assuming that the phonons (lattice) will not be affected by the magnetic field (no magneto vibronic effect), these latter data (high magnetic field) could be used as background for the other fields (including zero), and extract the magnetic part of the specific heat (see Figure 8, lower frame). Following this procedure, the magnetic part of the specific heat shows a peak at 9 K, which decreases in intensity with the application of the external magnetic field. The total value of the magnetic specific heat is rather low (0.1 J/mol K^2), indicating a very disordered system with a freezing temperature. This peak in the magnetic specific heat coincides with that observed in a.c. and d.c. magnetic susceptibility, indicating that the three techniques are exploring the same magnetic process. The error expected with this procedure to obtain the magnetic part of the specific heat could be 10−15%. The integration of this peak (magnetic entropy) is shown in the inset of the lower frame; the total entropy is much lower than that expected for 2 Mn^{4+} and Co^{2+} ($s = 2(\mathrm{Rln}(2S + 1))$), showing again that the system is disordered (or partially

ordered). The magnetic properties in $Sr_4Mn_2CoO_9$ system are rather similar to those obtained for $Sr_{3.3}Ca_{0.7}CoRh_2O_9$,[9] however in the former case the peaks in the specific heat and magnetic susceptibility are more pronounced, probably due to the ordered cationic distribution in $Sr_4Mn_2CoO_9$.

From the above presented magnetic and thermal properties, the picture that we could obtain for the $Sr_4Mn_2CoO_9$ system is that of a spin glass system, with strong frequency dependence below the freezing temperature, as well as a clear shift of this temperature with frequency. The freezing temperature (9.5 K) is obtained from the specific heat and magnetic susceptibility measurements, but the entropy associated with this partial order of the magnetic ions is much smaller than the entropy of the ordered state.

Acknowledgment. Financial support through research projects MAT2001-1440 and MAT2002-1329 (MCyT, Spain) is acknowledged.

CM034130T